

Flow Around an Automobile Wheel

FLUENT is used in this example to study the flow around an automotive wheel. To better understand the effect of rotation, the wheel is simulated with and without this motion. In both cases, the road and incoming air are given boundary conditions consistent with forward motion of the vehicle. The results are in good agreement with laboratory measurements taken from the literature.

The underbody airflow of an automobile is complicated by the presence of rotating wheels inside the wheel arches. Wheel rotation affects the drag and lift forces, vehicle stability, and passenger compartment noise level. It causes the oncoming air stream to be forced forward, down, and sideways from the front of each wheel. In this example, FLUENT is used to model this complex flow behavior. The simulation results are compared with the experimental results of Skea and Bullen [Ref. 1].

The geometry of the wheel and roadway is taken from the

experimental setup described in Ref. 1. A single wheel is considered, positioned alone on the road without a wheel arch or vehicle. As in the experiments, the wheel is modeled as a cylinder with a diameter of 400mm and width of 200mm. A 50mm long (flattened) patch of wheel is in contact with the ground. The wheel is placed in a rectangular domain, 5.55m in length, 2.16m in height and 4.778m in width. The large size of the domain ensures that the free-stream flow is

negligibly affected by the presence of the wheel. Using an incoming air stream, simulations are run with the wheel rotating and at rest.

Figure 1 shows the surface mesh on the wheel, a

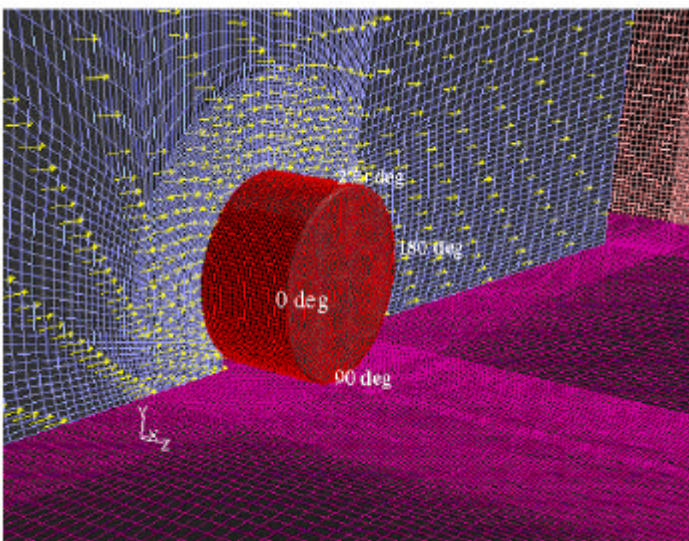


Figure 1: The surface grid used for the simulation and velocity vectors for the non-rotating case

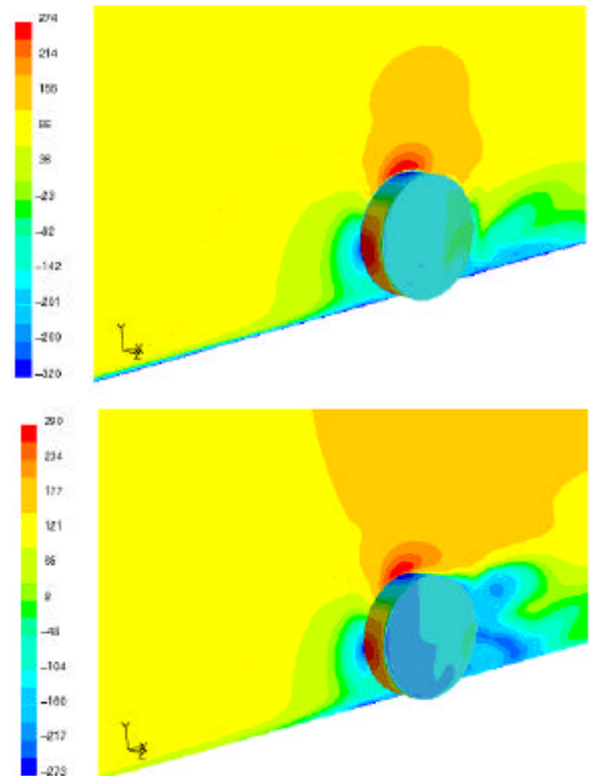


Figure 2: Velocity and pressure contours on the mid-plane and wheel, respectively, for the non-rotating (top) and rotating (bottom) wheel cases

vertical plane through one edge of the wheel, and the road. A structured hex mesh is used throughout the domain. The mesh is fine at the wheel walls and becomes coarser in the free-stream area. The total cell count is 1.87 million. A 20.4m/s (45.63mph) velocity is prescribed at the inlet while a constant (relative) pressure of 0 atm is prescribed at the outlet. The top

and side surfaces are treated as symmetry (zero normal gradient) boundaries. Wheel rotation is modeled by prescribing a rotational speed of 102rad/s (974rpm) to the cylindrical and side surfaces of the wheel. This corresponds to a speed over the road of 20.4m/s, consistent with the oncoming air stream. The road is also given a 20.4m/s velocity boundary condition, in keeping with the actual conditions experienced by the wheel. The RNG k-ε turbulence model is used with a standard wall function for turbulence modeling. The simulations are run until the velocity at a monitoring point in the wake of the wheel becomes constant. Velocity vectors in Figure 1 show the flow pattern around the wheel for the non-rotating case studied.

Figure 2 shows velocity contours on a vertical plane that bisects the wheel along with the pressure distribution on the wheel itself for the cases where the wheel is not rotating (top) and rotating (bottom). The contour scale in

each figure represents pressure values in Pascals. The effect of wheel rotation on flow separation is clearly seen from a comparison of the results. In particular, when the wheel rotates, boundary layer separation occurs earlier than when the wheel is at rest, resulting in a larger wake behind the wheel.

The pressure coefficient,

$$C_p = \frac{P_{static} - P_{ref}}{\frac{1}{2} \rho v^2}$$

around the circumference of the wheel is a more rigorous indicator of the effect of wheel rotation on the downstream flow. In Figure 3, C_p is shown for the stationary (left) and rotating (right) wheel. As indicated in Figure 1, 0° is at the front of the wheel, 90° is at the center of its contact with the road, 180° is behind the wheel, and so on. As expected, the pressure coefficient is highest at the front of the wheel and lowest directly behind it for both cases. With a few exceptions, the FLUENT results are in very good

agreement with the experimental values. Between 100 to 250°, C_p is more steady for a rotating wheel than it is for the non-rotating wheel, where a decreasing trend is evident.

In summary, FLUENT has been used in this example to study the flow over the wheel of an automobile. To understand the effect of the wheel rotation, two conditions were considered: in an oncoming air stream, the wheel was either at rest or rotating at a speed consistent with the speed of the oncoming air. Results were found to be in good agreement with experimental results found in the literature [Ref. 1]. More comprehensive studies could be performed that include the wheel housing, vehicle underbody, and the other nearby wheels.

Reference:

1. A. F. Skea and P. R. Bullen, *CFD Simulations and Experimental Measurements of the Flow Over a Rotating Wheel in a Wheel Arch*, SAE Paper No. 2001-01-0487, 2000.

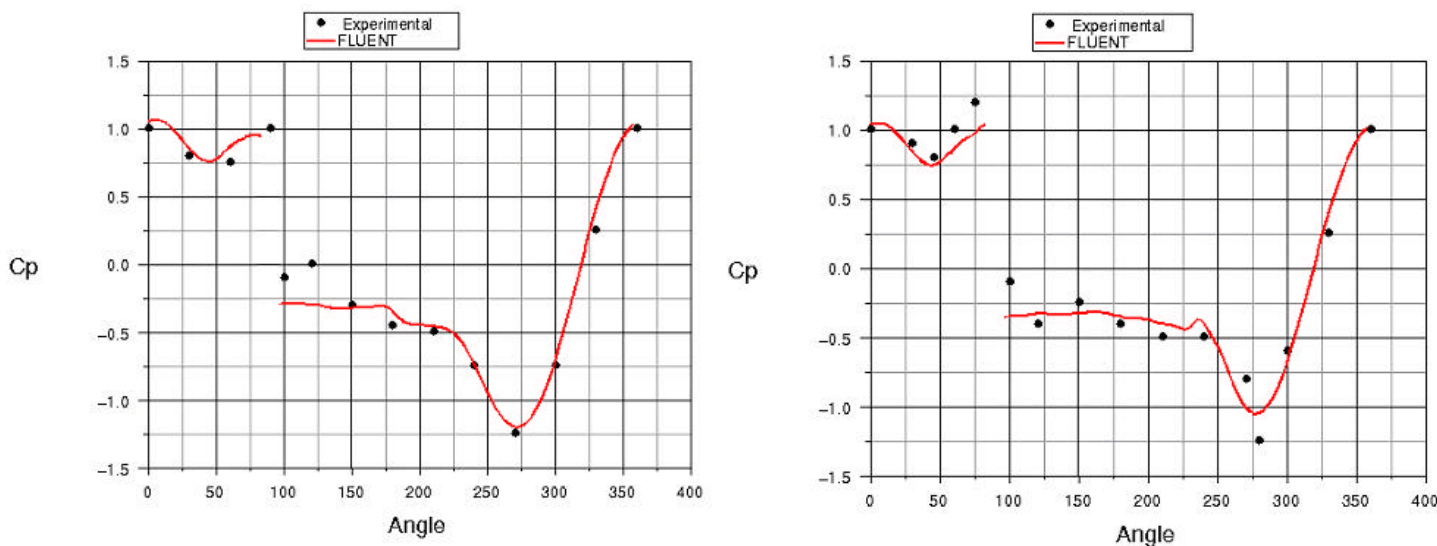


Figure 3: Pressure coefficient along the wheel perimeter for the non-rotating(left) and rotating (right) wheel cases